TCG-S: Orthogonal Coupling of P*-admissible Representations for General Floorplans [*]

Jai-Ming Lin[1] and Yao-Wen Chang[2]

[1]Department of Computer and Information Science, National Chiao Tung University, Hsinchu 300, Taiwan

[2]Department of Electrical Engineering & Graduate Institute of Electronics Engineering, National Taiwan University, Taipei 106, Taiwan

Abstract

We extend in this paper the concept of the P-admissible floorplan representation to that of the P*-admissible one. A P*-admissible representation can model the most general floorplans. Each of the currently existing P*-admissible representations, SP, BSG, and TCG, has its strengths as well as weaknesses. We show the equivalence of the two most promising P*-admissible representations, TCG and SP, and integrate TCG with a packing sequence (part of SP) into a new representation, called *TCG-S*. TCG-S combines the advantages of SP and TCG and at the same time eliminates their disadvantages. With the property of SP, faster packing and perturbation schemes are possible. Inherited nice properties from TCG, the geometric relations among modules are transparent to TCG-S (implying faster convergence to a desired solution), placement with position constraints becomes much easier, and incremental update for cost evaluation can be realized. These nice properties make TCG-S a superior representation which exhibits an elegant solution structure to facilitate the search for a desired floorplan/placement. Extensive experiments show that TCG-S results in the best area utilization, wirelength optimization, convergence speed, and stability among existing works and is very flexible in handling placement with special constraints.

1 Introduction

As technology advances, the circuit size in modern VLSI design increases dramatically. To handle the increasing design complexity, hierarchical designs and IP modules are widely used to optimize area and timing for design convergence. Further, the need to integrate heterogeneous systems or special modules imposes some placement constraints, e.g., the boundary-module constraint which requires some modules to be placed along the chip boundaries for shorter connections to pads, the preplaced-module constraint which pre-assigns modules to specific positions, etc. These trends make floorplanning/placement much more important than ever, and it is of particular significance to consider the floorplanning/placement with various constraints. To cope with these challenges, it is desired to develop an efficient and effective floorplan representation that can model the geometric relations among regular as well as constrained modules.

Many floorplan representations have been proposed in the literature, e.g., slicing tree [13], normalized Polish expression (NPE) [18], Sequence Pair (SP) [10], Bounded-Sliceline Grid (BSG) [12], O-tree [3], B*-tree [1], Corner Block List (CBL) [4], Transitive Closure Graph (TCG) [8], and Q-sequence [15]. Unlike the traditional classification of the slicing and non-slicing structures, we can alternatively classify them into two categories, *P*-admissible* and *non-P*-admissible* representations. A representation is said to be P-admissible if it satisfies the following four conditions [10]: (1) the solution space is finite, (2) every solution is feasible, (3) packing and cost evaluation can be performed in polynomial time, and (4) the best evaluated packing in the space corresponds to an optimal placement. We extend in this paper the concept of the P-admissible representation to that of the P*-admissible one by adding the fifth condition: (5) the geometric relation between each pair of modules is defined in the representation. With this condition, general floorplans/placements can be modeled. Therefore, a P*-admissible representation contains a complete structure for searching for an optimal floorplan/placement solution. Therefore, it is desirable to develop an effective and flexible P*-admissible representation.

Among the existing popular representations, SP, BSG, and TCG are P*-admissible while slicing tree, NPE, O-tree, B*-tree, CBL, and Q-sequence are not. The slicing tree and NPE are intended for slicing floorplans only. Since an optimal placement could be a non-slicing structure, the two representations are not P-admissible and thus not P*-admissible (i.e., violation of P*-admissibility Condition (4)). An O-tree defines only one-dimensional geometrical relation between *compacted* modules and thus can obtain the relation in the other dimension only after packing (i.e., violation of Condition (5)). (Note that O-tree is undefined for some uncompacted placements which may correspond to the best solutions for wirelength optimization. Therefore, as far as wirelength optimization is concerned, O-tree is not even P-admissible since Condition (4) is violated.) A B*-tree requires a placement to be left and/or bottom compacted. However, the space intended for placing a module may be occupied by previously placed modules during packing, resulting in a mismatch between the original representation and its *compacted* placement. Therefore, it may not be feasible to find a *compacted* placement corresponding to the original B*-tree, and thus it is not P-admissible (i.e., violation of Condition (2)). CBL and Q-sequence can represent only *mosaic* floorplans, in which each region in the floorplan contains exactly one module. CBL and Q-sequence are not P-admissible because it cannot guarantee a feasible solution after a perturbation (i.e., violation of Conditions (2) and (4)). Non-P*-admissible representations intrinsically have a smaller solution space and lower packing cost since their corresponding floorplanning/placement structures are more restricted (e.g., slicing structures [slicing tree, NPE], mosaic floorplans [CBL, Q-sequence], compacted placements [O-tree, B*-tree], etc).[1] However, lack of the definition on the geometric relation between each pair of modules, the guarantee in the feasibility, and/or the optimality of their representations would inevitably complicate floorplan sizing and placement with constraints, lead to longer running times, and/or lower solution quality.

The existing P*-admissible representations, SP, BSG, and TCG, have their own distinct properties as well as common ones. Nevertheless, researchers tend to favor SP over BSG because BSG incurs many redundancies and thus a much larger solution space, implying a longer running time to search for a good solution. Therefore, we shall focus on SP and TCG. Both SP and TCG are considered very flexible representations and construct constraint graphs to evaluate their packing cost. SP consists of two sequences of modules (Γ_+, Γ_-), where Γ_+ (Γ_-) specifies the module ordering from top-left (bottom-left) to bottom-right (top-right). Hence, Γ_- corresponds to the ordering for packing modules to the bottom-left direction and thus can be used to guide module packing. However, like most existing representations (e.g., NPE, BSG, O-tree, B*-tree, CBL, Q-sequence), the geometric relations between modules are *not transparent* to the operations of SP (i.e., the effect of an operation on the change of module relation is not clear before packing), and thus we need to construct constraint graphs from scratch after each perturbation to evaluate the packing cost; this deficiency makes SP harder to converge to a desired solution and to handle placement with constraints

[*]This work was partially supported by the National Science Council of Taiwan ROC under Grant No. NSC-89-2215-E-009-117. E-mails: gis87808@cis.nctu.edu.tw; ywchang@cc.ee.ntu.edu.tw.

[1]Generality from the most general to the least general: general floorplan $\succ$ compacted floorplan $\succ$ mosaic floorplan $\succ$ slicing floorplan.

(e.g., boundary modules, pre-placed modules, etc).

TCG consists of a horizontal transitive closure graph C_h to define the horizontal geometric relations between modules and a vertical one C_v for vertical geometric relations. Contrast to SP, the geometric relations between modules are transparent to TCG as well as its operations, facilitating the convergence to a desired solution. Further, TCG supports incremental update during operations and keeps the information of boundary modules as well as the shapes and the relative positions of modules in the representation. Nevertheless, like SP, constraint graphs are also needed for TCG to evaluate its packing cost, and unlike SP, we need to perform extra operations to obtain the module packing sequence.

Therefore, an interesting question arises: Is it possible to develop a representation that can combine the advantages of SP and TCG and at the same time eliminate their disadvantages? We answer this question in affirmation by showing the equivalence of TCG and SP, and integrating them into TCG-S = (C_h, C_v, Γ_-). The orthogonal combination leads to a representation with at least the following advantages:

- With the property of SP, faster $O(m \lg m)$-time packing and $O(m)$-time perturbation schemes are possible for a P*-admissible representation, where m is the number of modules. (Note that a linear-time packing scheme is possible for the tree-based representations, but they can represent only more restricted compacted floorplans.)
- Inherited from TCG, the geometric relations among modules are transparent to TCG-S, implying faster convergence to a desired solution.
- Inherited from TCG, placement with position constraints becomes much easier.
- TCG-S can support incremental update for cost evaluation.

These nice properties make TCG-S an effective, efficient, and flexible representation. Extensive experiments based on a set of commonly used MCNC benchmarks show that TCG-S results in the best area utilization, wirelength optimization, convergence speed, and solution stability among existing works.

To show the flexibility of TCG-S, we also consider placement with preplaced and boundary modules. For placement with pre-placed modules, Murata et al. [11] proposed an *adaptation algorithm* to transform an infeasible SP with preplaced modules into a feasible one. However, the process incurs expensive computations. For placement with the boundary-module constraint, Tang and Wong in [16] and Ma et al. in [9] handled this problem using SP and CBL, respectively. However, they cannot guarantee a feasible solution in each perturbation and their final placements. Lai et al. in [6] gave the feasibility conditions for SP with boundary modules and transformed an infeasible solution into a feasible one. However, the method is very complex, and many rules are needed to cope with the constraints .

We present in this paper the methods for handling placement with preplaced and boundary modules. Different from the previous works on boundary modules that cannot guarantee a feasible solution or need to transform an infeasible solution into a feasible one, TCG-S can easily maintain the feasibility during each perturbation. We compared our work with [6] on placement with boundary modules. (Note that there are no common benchmark circuits for this constraint.) Experimental results show that TCG-S results in smaller areas than [6].

The remainder of this paper is organized as follows. Section 2 formulates the floorplan/placement design problem. Section 3 compares SP and TCG. Section 4 presents the procedures to build the TCG-S from a placement and construct the placement from a TCG-S. Section 5 gives the operations to perturb a TCG-S. Section 6 presents our methods to handle placement with boundary and preplaced modules. Experimental results are reported in Section 7. Finally, we give concluding remarks in Section 8.

2 Problem Definition

Let $B = \{b_1, b_2, ..., b_m\}$ be a set of m rectangular modules whose width, height, and area are denoted by W_i, H_i, and A_i, $1 \le i \le m$. Let (x_i, y_i) $((x'_i, y'_i))$ denote coordinate of the bottom-left (top-right) corner of module b_i, $1 \le i \le m$, on a chip. A placement $\mathcal{P}$ is an assignment of (x_i, y_i) for each b_i, $1 \le i \le m$, such that no two modules overlap. The goal of floorplanning/placement is to optimize a predefined cost metric such as a combination of the area (i.e., the minimum bounding rectangle of $\mathcal{P}$) and/or the wirelength (i.e., the summation of half bounding box of interconnections) induced by the assignment of b_i's on the chip.

3 P*-admissible Representations

In this section, we first review the two P*-admissible representations, TCG and SP, then show their equivalence, and compare their properties.

3.1 Review of TCG and SP

TCG describes the geometric relations between modules based on two graphs, namely a *horizontal transitive closure graph* C_h and a *vertical transitive closure graph* C_v, in which a node n_i represents a module b_i and an edge (n_i, n_j) in C_h (C_v) denotes that module b_i is left to (below) module b_j. TCG has the following three *feasibility properties* [8]:

1. C_h and C_v are acyclic.
2. Each pair of nodes must be connected by exactly one edge either in C_h or in C_v.
3. The transitive closure of C_h (C_v) is equal to C_h (C_v) itself.[2]

Figure 1(a) shows a placement with seven modules a, b, c, d, e, f, and g whose widths and heights are (3.5, 1.5), (2, 2.5), (2, 3.5), (3, 2), (1.5, 1.5), (5, 1.5), and (1, 2), respectively. Figure 1(c) shows the TCG $= (C_h, C_v)$ corresponding to the placement of Figure 1(a). The value associated with a node in C_h (C_v) gives the width (height) of the corresponding module, and the edge (n_i, n_j) in C_h (C_v) denotes the horizontal (vertical) relation of b_i and b_j. Since there exists an edge (n_a, n_g) in C_h, module b_a is left to b_g. Similarly, b_a is below b_b since there exists an edge (n_a, n_b) in C_v.

SP uses a pair of sequences (Γ_+, Γ_-) to represent a floorplan/placement, where Γ_+ and Γ_- give two permutations of module names. The geometric relation of modules can be derived from an SP as follows. Module b_a is left (right) to module b_b if a appears before (after) b in both Γ_+ and Γ_-. Module b_a is below (above) module b_b if b appears before (after) a in Γ_+ and a appears before (after) b in Γ_-. Figure 1(b) shows the corresponding SP. Since a is before g in both Γ_+ and Γ_-, module b_a is left to module b_g. Similarly, b_a is below b_b since a is after b in Γ_+ and before b in Γ_-.

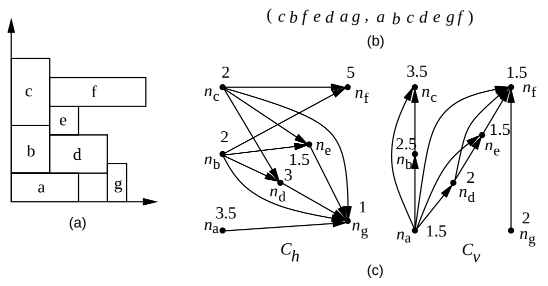

Figure 1: (a) A placement. (b) The corresponding SP of (a). (c) The corresponding TCG of (a).

3.2 Equivalence of SP and TCG

Like the relations between a skewed slicing tree [13] and an NPE [18] for slicing floorplans as well as O-tree and B*-tree for non-slicing floorplans, TCG and SP are equivalent.

We can transform between TCG and SP as follows: Let the *fan-in* (*fan-out*) of a node n_i, denoted by $F_{in}(n_i)$ $(F_{out}(n_i))$, be the nodes n_j's with edges (n_j, n_i) $((n_i, n_j))$. Given a TCG, we can obtain a sequence Γ_+ by repeatedly extracting a node n_i with $F_{in}(n_i) = \emptyset$ in C_h and $F_{out}(n_i) = \emptyset$ in C_v, and then deleting the edges (n_i, n_j)'s $((n_j, n_i)$'s) from C_h (C_v) until no node is left in C_h (C_v). Similarly, we can transform a TCG into another sequence Γ_- by repeatedly extracting the node n_i with $F_{in}(n_i) = \emptyset$ both in C_v and C_h, and then deleting the edges (n_i, n_j)'s from both C_h and C_v until no node is left in C_h and C_v. Given an SP = (Γ_+, Γ_-), we can obtain a unique TCG = (C_h, C_v) from the two constraint graphs of the SP by removing the source, sink, and associated edges. For example, the SP of Figures 1(b) is equivalent to the TCG of Figures 1(c).

[2]The transitive closure of a directed acyclic graph G is defined as the graph $G' = (V, E')$, where E' =$\{(n_i, n_j)$: there is a path from node n_i to node n_j in $G\}$.

3.3 Comparison between TCG and SP

Although TCG and SP are equivalent, their properties and induced operations are significantly different. (Similar situations are also with skewed slicing trees/NPE's and O-trees/B*-trees.) Both SP and TCG are considered very flexible representations and construct constraint graphs to evaluate their packing cost. Γ_- of an SP corresponds to the ordering for packing modules to the bottom-left direction and thus can be used for guiding module packing. However, like most existing representations, the geometric relations among modules are not transparent to the operations of SP (i.e., the effect of an operation on the change of module relation is not clear before packing), and thus we need to construct constraint graphs from scratch after each perturbation to evaluate the packing cost; this deficiency makes SP harder to converge to a desired solution and to handle placement with constraints (e.g., boundary modules, pre-placed modules, etc).

Contrast to SP, the geometric relations among modules are transparent to TCG as well as its operations, facilitating the convergence to a desired solution. Further, TCG supports incremental update during operations and keeps the information of boundary modules as well as the shapes and the relative positions of modules in the representation. Unlike SP, nevertheless, we need to perform extra operations to obtain the module packing sequence and an additional $O(m^2)$ time to find a special type of edges, called *reduction edges*, in C_h (C_v) for some operations. (We will define the edges later.)

For both SP and TCG, the packing scheme by applying the longest path algorithm is time-consuming since all edges in the constraint graphs are processed, even though they are not on the longest path. As shown in C_h of Figure 1(c), if we add a source with zero weight and connect it to those nodes with zero in-degree, the x coordinate of each module can be obtained by applying the longest path algorithm on the resulting directed acyclic graph. Therefore, we have $x_g = \max\{x'_a, x'_b, x'_c, x'_d, x'_e\}$. However, if we place modules based on the sequence Γ_- and maintain a horizontal and a vertical contours, denoted by R_h and R_v respectively, for the placed modules, the number of nodes need to be considered can be reduced. Let R_h (R_v) be a list of modules b_i's for which there exists no module b_j with $y_j \geq y'_i$ ($x_j \geq x'_i$) and $x'_j \geq x'_i$ ($y'_j \geq y'_i$). For the placement of Figure 1(a), for example, $R_h =< b_c, b_f >$ and $R_v =< b_g, b_d, b_e, b_f, b_c >$. Suppose we have packed the modules b_a, b_b, b_c, b_d, and b_e based on the sequence Γ_-. Then, the resulting horizontal contour $R_h =< b_c, b_e, b_d >$. Keeping R_h, we only need to traverse the contour from b_e, predecessors of b_e, to the last module b_d, which have horizontal relations with b_g (since there are edges (n_e, n_g) and (n_d, n_g) in C_h). Thus, we have $x_g = x'_d$. Packing modules in this way, we only need to consider x_e and x_d, and can get rid of the computation for a maximum value, leading to a faster packing scheme. We will show later how to apply a balanced binary tree to implement the contour operation to get a loglinear-time packing scheme.

4 The TCG-S Representation

Combining TCG $= (C_h, C_v)$ and SP $= (\Gamma_+, \Gamma_-)$, we develop a representation, called TCG-S $= (C_h, C_v, \Gamma_-)$, which uses a horizontal and a vertical transitive closure graphs as well as a packing sequence Γ_- to represent a placement. In this section, we first introduce how to construct Γ_-, C_h, and C_v from a placement. Then, we propose an $O(m \lg m)$-time packing scheme for TCG-S, where m is the number of modules.

4.1 From a placement to TCG-S

In this subsection, we first extract Γ_- from a placement, and then construct C_h and C_v according to Γ_-.

For two non-overlapped modules b_i and b_j, b_i is said to be *horizontally* (*vertically*) *related* to b_j, denoted by $b_i \vdash b_j$ ($b_i \perp b_j$), if b_i is left to (below) b_j and their projections on the y (x) axis overlap. For two non-overlapped modules b_i and b_j, b_i is said to be *diagonally related* to b_j if b_i is left to b_j and their projections on the x and the y axes do not overlap. To simplify the operations on geometric relations, a diagonal relation for modules b_i and b_j is treated as a horizontal one unless there exists a chain of vertical relations from b_i (b_j), followed by the modules overlapped with the rectangle defined by the two closest corners of b_i and b_j, and finally to b_j (b_i), for which it is considered as $b_i \perp b_j$ ($b_j \perp b_i$).

Given a placement, Γ_- can be extracted based on the procedure described in [10]. For example, the Γ_- for the placement of Figure 2(a) is $< abcdegf >$. After extracting Γ_-, we can construct C_h and C_v based on Γ_-. For each module b_i in Γ_-, we introduce a node n_i with the weight being b_i's width (height) in C_h (C_v). Also, for each module b_i before b_j in Γ_-, we introduce an edge (n_i, n_j) in C_h (C_v) if $b_i \vdash b_j$ ($b_i \perp b_j$). As shown in Figures 2(b), for the first two modules b_a, b_b in Γ_-, we introduce the nodes n_a and n_b in C_h (C_v) and assign the weights as their widths (heights). Also, we construct a directed edge (n_a, n_b) in C_v since module b_a is before b_b and $b_a \perp b_b$. The process repeats for all modules in Γ_-, resulting in the TCG-S shown in Figure 2(b). We have the following theorem.

Theorem 1 *There exists a TCG-S corresponding to a placement.*

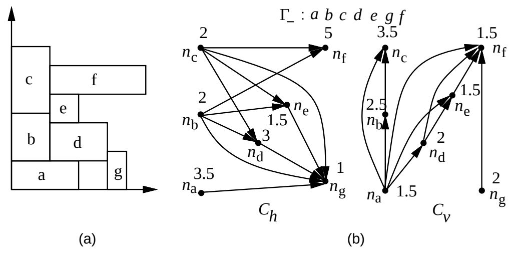

Figure 2: (a) A placement. (b) The corresponding TCG-S of (a).

4.2 From TCG-S to a placement

In this subsection, we propose an $O(m \lg m)$-time packing scheme based on Γ_- as well as a horizontal and a vertical contours R_h and R_v, where m is the number of modules. The basic idea is to process the modules based on the sequence defined in Γ_-, and then pack the current module to a corner formed by two previously placed modules in R_h (R_v) according to the geometric relations defined in C_h and C_v.

We detail the packing scheme as follows. Recall that R_h (R_v) is a list of modules b_i's for which there exists no module b_j with $y_j \geq y'_i$ ($x_j \geq x'_i$) and $x'_j \geq x'_i$ ($y'_j \geq y'_i$). (R_h (R_v) consists of modules along the top (left) boundary of a placement.) We can keep the modules b_i's in R_h (R_v) in a balanced binary search tree (e.g., the red-black tree [2]) T_h (T_v) in the increasing order according to their right (top) boundaries. For easier presentation, we add a *dummy module* b_s (b_t) to R_h (R_v) to denote the left (bottom) boundary module of a placement. We have $b_s \vdash b_i$ and $b_t \perp b_i, \forall b_i$. Let $(x'_s, y'_s) = (0, \infty)$ and $(x'_t, y'_t) = (\infty, 0)$. R_h (R_v) consists of b_s (b_t) initially, and so does the corresponding T_h (T_v). To pack a module b_j in Γ_-, we traverse the modules b_k's in T_h (T_v) from its root, and go to the right child if $b_k \vdash b_j$ ($b_k \perp b_j$) and the left child if $b_k \perp b_j$ ($b_k \vdash b_j$). The process is repeated for the newly encountered module until a leaf node is met. Then, b_j is connected to the leaf node, and $x_j = x'_p$ ($y_j = y'_p$), where b_p is the last module with $b_p \vdash b_j$ ($b_p \perp b_j$) in the path. After b_j is inserted into T_h (T_v), every predecessor b_l with $x'_l \leq x'_j$ ($y'_l \leq y'_j$) in T_h (T_v) is deleted since b_l is no longer in the contour. (Note that the ordering of nodes in T_h (T_v) can be obtained by depth-first search.) This process repeats for all modules in Γ_-. We have $W = x'_v$ ($H = y'_v$) if b_v is the module in the resulting T_h (T_v) with the largest value, where W (H) denotes the width (height) of the placement. We have the following theorems and lemmas.

Theorem 2 *There exists a unique placement corresponding to a TCG-S.*

Lemma 1 *For each module b_i in Γ_-, b_i must be placed adjacent to the right (top) boundary of some module b_j in R_h (R_v) during the packing.*

Lemma 2 *Given a module b_i in Γ_- to be placed, if $b_j \in R_h(R_v)$, $b_j \perp b_i$ ($b_j \vdash b_i$), and b_j has the largest x'_j (y'_j), any module $b_k \in R_h(R_v)$ with $x'_k > x'_j$ ($y'_k > y'_j$)) cannot have the relation $b_k \vdash b_i$ ($b_k \perp b_i$).*

Theorem 3 *The proposed scheme correctly packs all modules in $O(m \lg m)$ time, where m is the number of modules.*

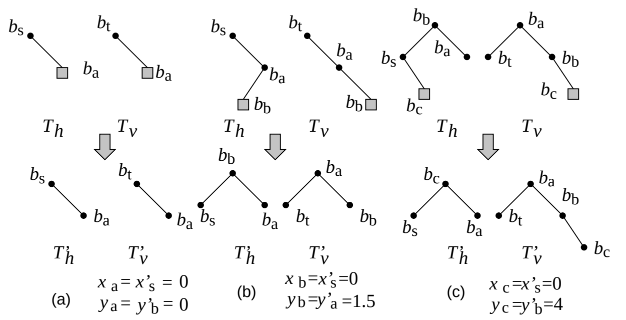

T_h
T_v
T'_h
T'_v
(a) $x_a = x'_s = 0$, $y_a = y'_b = 0$
(b) $x_b = x'_s = 0$, $y_b = y'_a = 1.5$
(c) $x_c = x'_s = 0$, $y_c = y'_b = 4$

Figure 3: The packing scheme for the TCG-S of Figure 2(b).

Figures 3 shows the packing scheme for the TCG-S of Figure 2(b). T_h (T_v) consists of b_s (b_t) initially. To pack the first module b_a in Γ_-, we traverse T_h (T_v) from the root b_s (b_t) and insert it to the right child of b_s (b_t) since $b_s \vdash b_a$ ($b_t \perp b_a$). Therefore, the first module b_a in Γ_- is placed at the bottom-left corner (i.e., $(x_a, y_a) = (0, 0)$) since b_s (b_t) is the last module that is horizontally (vertically) related to b_a and $x'_s = 0$ ($y'_t = 0$). (Note that T'_h (T'_v) in Figures 3(a) denotes a balanced binary search tree after b_a is inserted into T_h (T_v).) Similarly, to pack the second module b_b in Γ_-, we traverse T_h from the root b_s and then its right child since $b_s \vdash b_b$. Then, b_b is inserted to the left child of b_a since $b_s \perp b_a$. Because b_s is the last module with $b_s \vdash b_b$ in the path, $x_b = x'_s = 0$. Similarly, we traverse T_v from the root b_t and then its right child b_a since $b_a \perp b_t$. Then, b_b is inserted to the right child of b_a in T_v since $b_a \perp b_b$. Therefore, $y_b = y'_a = 1.5$ because b_a is the last module with $b_a \perp b_b$ in the path. The resulting balanced binary search trees after performing tree rotations T'_h, T'_v are shown in Figure 3(b) (see [2] for the rotation operations for keeping a tree balanced). As shown in Figure 3(c), after b_c is inserted, b_b in T_h is deleted since b_b is a predecessor of b_c and $x'_b \leq x'_c$ (i.e., b_b is no longer in the contour). The resulting T'_h and T'_v are shown in Figure 3(c). The process is repeated for all modules in Γ_-.

According to this packing scheme, if the coordinate of a module b_i in Γ_- is changed, we only need to recompute the coordinates of modules after b_i in Γ_- since the coordinates of modules before b_i do not change.

5 Floorplanning Algorithm

We develop a simulated annealing based algorithm [5] by using TCG-S for general floorplan design. Given an initial TCG-S, the algorithm perturbs the TCG-S into a new TCG-S to find a desired solution. To ensure the correctness of the new C_h and C_v, they must satisfy the three feasibility conditions given in Section 3.1. To identify feasible C_h and C_v for perturbation, we describe the concept of *reduction edges* in the following subsection.

5.1 Reduction Edge

An edge (n_i, n_j) is said to be a *reduction edge* if there does not exist another path from n_i to n_j, except the edge (n_i, n_j) itself; otherwise, it is a *closure edge*, for some operations. In Figure 2(b), for example, edges (n_a, n_g), (n_d, n_g), and (n_e, n_g) are reduction edges while (n_b, n_g) and (n_c, n_g) are closure ones. With Γ_-, we can find a *set* of reduction edges in $O(m)$ time (where m is the number of modules), a significant improvement from $O(m^2)$ time using TCG alone [8].

Given an arbitrary node n_i in a transitive closure graph C_h (C_v), we can find all the nodes n_j's that form reduction edges (n_i, n_j)'s using a *Linear Scan* method as follows. First, we extract from Γ_- those nodes n_j's in $F_{out}(n_i)$ of C_h (C_v) and keep their original ordering in Γ_-. Let the resulting sequence be S. The first node n_k in S and n_i must form a reduction edge (n_i, n_k). Then, we continue to traverse S until a node n_l with (n_k, n_l) *not* in C_h (C_v) is encountered. (n_i, n_l) must also be a reduction edge. Starting from n_l, we continue the same process until no node is left in S.

As an example shown in C_h of Figure 2(b), we are to extract all reduction edges emanating from n_c. We first find $S =< n_d, n_e, n_g, n_f >$ by extracting nodes in $F_{out}(n_c)$ based on the sequence in Γ_-. n_c and the first node n_d in S form a reduction edge (n_c, n_d). Traversing S, we have another reduction edge (n_c, n_e) since edge (n_d, n_e) is not in C_h. Starting from n_e, we search the next node n with (n_e, n) not in C_h. We find node n_f, implying that (n_c, n_f) is also a reduction edge. Therefore, we have found all reduction edges emanating from n_c: (n_c, n_d), (n_c, n_e), and (n_c, n_f). (Note that (n_c, n_g) is not a reduction edge because we found (n_e, n_g) in C_h during the processing.)

Theorem 4 *Given a node n_i in C_h (C_v), the Linear Scan method finds all reduction edges emanating from n_i in $O(m)$ time, where m is the number of modules.*

5.2 Solution Perturbation

We extend the four operations *Rotation*, *Swap*, *Reverse*, and *Move* presented in [8] to perturb C_h and C_v. During each perturbation, we must maintain the three feasibility properties for C_h and C_v. Unlike the Rotation operation, Swap, Reverse, and Move may change the configurations of C_h and C_v and thus their properties. Further, we also need to maintain Γ_- to conform to the topological ordering of the new C_h and C_v.

5.2.1 Rotation

To Rotate a module b_i, we exchange the weights of the corresponding node n_i in C_h and C_v. Since the configurations of C_h and C_v do not change, so dose Γ_-. Figure 4(a) shows the resulting TCG-S after rotating the module g shown in Figure 2(b). Notice that the new Γ_- is the same as that in Figure 4(a).

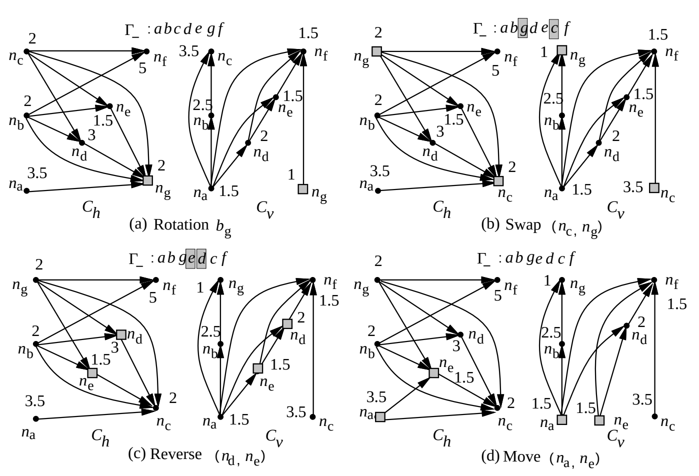

Γ_- : $a\,b\,c\,d\,e\,g\,f$
(a) Rotation b_g
Γ_- : $a\,b\,g\,d\,e\,c\,f$
(b) Swap (n_c, n_g)
Γ_- : $a\,b\,g\,e\,d\,c\,f$
(c) Reverse (n_d, n_e)
Γ_- : $a\,b\,g\,e\,d\,c\,f$
(d) Move (n_a, n_e)
C_h
C_v

Figure 4: Four types of perturbation. (a) The resulting TCG-S after rotating the module b_g shown in Figure 2(b). (b) The resulting TCG-S after swapping the nodes n_c and n_g shown in (a). (c) The resulting TCG-S after reversing the reduction edge (n_d, n_e) shown in (b). (d) The resulting TCG-S after moving the reduction edge (n_a, n_e) from the C_v of (c) to C_h.

5.2.2 Swap

Swapping n_i and n_j does not change the topologies of C_h and C_v, except that nodes n_i and n_j in both C_h and C_v are exchanged. Therefore, we only need to exchange b_i and b_j in Γ_-. Figure 4(b) shows the resulting TCG-S after swapping the nodes n_c and n_g shown in Figure 4(a). Notice that the modules b_c and b_g in Γ_- in Figure 4(b) are exchanged.

5.2.3 Reverse

Reverse changes the geometric relation between b_i and b_j from $b_i \vdash b_j$ ($b_i \perp b_j$) to $b_j \vdash b_i$ ($b_j \perp b_i$). To reverse a reduction edge (n_i, n_j) in one transitive closure graph, we first delete the edge (n_i, n_j) from the graph, and then add the edge (n_j, n_i) to the graph. To keep C_h and C_v feasible, for each node $n_k \in F_{in}(n_j) \cup \{n_j\}$ and $n_l \in F_{out}(n_i) \cup \{n_i\}$ in the new graph, we have to keep the edge (n_k, n_l) in the new graph. If the edge does not exist in the graph, we add the edge to the graph and delete the corresponding edge (n_k, n_l) (or (n_l, n_k)) in the other graph. To make Γ_- conform to the topological ordering of the new C_h and C_v, we delete b_i from Γ_- and insert b_i after b_j. For each module b_k between b_i and b_j in Γ_-, we shall check whether the edge (n_i, n_k) exists in the same graph. We do nothing if the edge (n_i, n_k) does not exist in the same graph; otherwise, we delete b_k from Γ_- and insert it after the most recently inserted module.

Figure 4(c) shows the resulting TCG-S after reversing the *reduction edge* (n_d, n_e) of the C_v in Figure 4(b). Since there exists no module between b_d and b_e in Γ_-, we only need to delete b_d from Γ_- and insert it after b_e, and the resulting Γ_- is shown in Figure 4(c).

5.2.4 Move

Move changes the geometric relation between b_i and b_j from $b_i \vdash b_j$ ($b_i \perp b_j$) to $b_i \perp b_j$ ($b_i \vdash b_j$). To move a reduction edge (n_i, n_j) from a transitive closure graph G to the other G', we delete the edge from G and then add it to G'. Similar to Reverse, for each node $n_k \in F_{in}(n_i) \cup \{n_i\}$ and $n_l \in F_{out}(n_j) \cup \{n_j\}$ in G', we must move the edge (n_k, n_l) to G' if the the corresponding edge (n_k, n_l) (or (n_l, n_k)) is in G. Since the operation changes only the edges in C_h or C_v but not the topological ordering among nodes, Γ_- remains unchanged.

Figure 4(d) shows the resulting TCG-S after moving the *reduction edge* (n_a, n_e) from C_v to C_h in Figure 4(c). Notice that the resulting Γ_- is the same as that in Figure 4(c).

For the above operations, Rotation and Move do not change the topological ordering of Γ_- while Swap and Reverse need respective $O(1)$ and $O(m)$ times to maintain the topological ordering of Γ_-, where m is the number of modules. We have the following theorem.

Theorem 5 *TCG-S is closed under the Rotation, Swap, Reverse, and Move operations.*

In particular, it suffices to apply the four perturbations to explore the whole solution space. Extending the similar work by [17] for TCG, we have the following theorem.

Theorem 6 *Given two arbitrary TCG-S's S_1 and S_2, we can obtain S_2 from S_1 by applying a finite number of Rotation, Swap, Reverse, and Move operations, and vice versa.*

6 Placement with Constraints

In this section, we demonstrate the flexibility of TCG-S by extending it to handle placement with boundary and pre-placed modules.

6.1 TCG-S with Boundary Modules

The placement with boundary constraints is to place a set of prespecified modules along the designated boundaries of a chip, which can be formulated as follows:

Definition 1 Boundary Constraint: *Given a boundary module b, it must be placed in one of the four sides: on the left, on the right, at the bottom or at the top in a chip in the final packing.*

TCG-S keeps the following properties that make placement with boundary constraints much easier than other representations.

Theorem 7 *If a module b_i is placed along the left (right) boundary, the in-degree (out-degree) of the node n_i in C_h equals zero. If a module b_i is placed along the bottom (top) boundary, the in-degree (out-degree) of node n_i in C_v equals zero.*

For each perturbation, we can guarantee a feasible placement by checking whether the conditions of boundary modules are satisfied. We discuss the modifications for the four perturbation operations as follows.

6.1.1 Rotation

Since Rotation does not change module location, the operation remains the same as before.

6.1.2 Swap

We can swap two nodes n_a and n_b if

1. b_a and b_b are not boundary modules,
2. b_a and b_b are boundary modules of the same type, or
3. b_a is a boundary module and b_b is not, and n_b satisfies the boundary constraint of b_a.

6.1.3 Reverse

If b_a is a left boundary module or b_b is a right boundary module, then the reduction edge (n_a, n_b) in C_h cannot be reversed. Similarly, we cannot reverse the reduction edge (n_a, n_b) in C_v if b_a is a bottom boundary module or b_b is a top boundary module

6.1.4 Move

If b_a is a top boundary module or b_b is a bottom boundary module, we cannot move the reduction edge (n_a, n_b) from C_h to C_v. Similarly, we cannot move the reduction edge (n_a, n_b) from C_v to C_h if b_a is a right boundary module or b_b is a left boundary module

We have the following theorem.

Theorem 8 *TCG-S is closed under the Rotation, Swap, Reverse, and Move operations with boundary constraints.*

6.2 TCG-S with Pre-placed Modules

The placement with pre-placed modules is to place a set of prespecified modules at the designated locations of a chip, which can be formulated as follows:

Definition 2 Pre-placed Constraint: *Given a module b_i with a fixed coordinate (x_i, y_i) and an orientation, b_i must be placed at the designated location with the same orientation in the final packing.*

Whether a pre-placed module is packed at a correct location is not known until packing. Also, changing the coordinate of a module b_i may affect the packing for other modules after b_i in Γ_-. Therefore, we may need to modify a TCG-S to guarantee a feasible placement with the pre-placed constraint after each perturbation.

Given a TCG-S, modules are packed one by one based on the sequence of Γ_-. A module b_i *interacts with* another module b_j if (1) b_i overlaps b_j, (2) $b_j \vdash b_i$ and their projections on the y axis overlap, or (3) $b_j \perp b_i$ and their projections on the x axis overlap. If b_i interacts with a pre-placed module b_j and b_j was not placed, n_i and n_j are swapped in the TCG-S to make b_j placed at the designated location. If a pre-placed module b_i was placed and the resulting placement of b_i does not interact with itself at the designated location, we swap b_i with the node b_j right after b_i in Γ_-; otherwise, b_i is placed at the designated location if there exists no module behind b_i in Γ_-.

7 Experimental Results

Based on a simulated annealing method [5], we implemented the TCG-S representation in the C++ programming language on a 433 MHz SUN Sparc Ultra-60 workstation with 1 GB memory. The source code is available at http://cc.ee.ntu.edu.tw/∼ywchang/research.html. Based on the five commonly used MCNC benchmark circuits, we conducted four experiments: (1) area optimization, (2) wirelength optimization, (3) solution convergence speed and stability, and (4) placement with boundary constraints. In Table 1, Columns 2 and 3 list the respective numbers of modules and nets of the five circuits.

For Experiment (1), the area and runtime comparisons among SP, O-tree, B*-tree, enhanced O-tree, CBL, and TCG are listed in Table 1. As shown in Table 1, TCG-S achieves the best area utilization for the benchmark circuits in very efficient running times. Figure 6 (left) shows the resulting placement for ami49 with area optimization.

For Experiment (2), we estimated the wirelength of a net by half the perimeter of the minimum bounding box enclosing the net. The wirelength of a placement is given by the summation of the wirelengths of all nets. As shown in Table 2, TCG-S achieves better average results in wirelength than O-tree, enhanced O-tree, and TCG in smaller running times. (Note that we did not compare with B*-tree and CBL here since they did not report the results on optimizing wirelength alone.)

In addition to the area and timing optimization, in Experiment(3), we also compared the solution convergence speed and stability among SP, TCG, and TCG-S to eliminate the possible unfairness due to the non-deterministic behavior of simulated annealing, which were neglected in most previous works. (Note that other tools are not available to us for the comparative study.) We randomly ran SP, TCG, and TCG-S on ami49 ten times based on the same initial placement whose area is $102mm^2$. The resulting areas are plotted as functions of the running times (sec). Figures 5(a), (b), and (c) show the resulting curves of SP, TCG, and TCG-S, respectively. To see the detailed convergence rates, we show in Figures 5 only the potions whose areas are smaller than 47 mm^2. As illustrated in Figure 5(c), TCG-S converges very fast to desired solutions, and the results are very stable (≤ 37.5 mm^2 for all runs). In contrast, the convergence speed of SP is much slower than TCG-S and TCG, and the resulting areas are often larger than 39 mm^2. Further, there

Circuit	# of modules	# of nets	SP		O-tree		B*-tree		Enhanced O-tree		CBL		TCG		TCG-S	
			Area mm^2	Time sec	Area mm^2	Time sec	Area mm^2	Time sec	Area mm^2	Time sec	Area mm^2	Time sec	Area mm^2	Time sec	Area mm^2	Time sec
apte	9	97	48.12	13	47.1	38	**46.92**	7	**46.92**	11	NA	NA	**46.92**	1	**46.92**	1
xerox	10	203	20.69	15	20.1	118	19.83	25	20.21	38	20.96	30	19.83	18	**19.796**	5
hp	11	83	9.93	5	9.21	57	**8.947**	55	9.16	19	(66.14)	(32)	**8.947**	20	**8.947**	7
ami33	33	123	1.22	676	1.25	1430	1.27	3417	1.24	118	1.20	36	1.20	306	**1.185**	84
ami49	49	408	38.84	1580	37.6	7428	36.80	4752	37.73	406	38.58	65	36.77	434	**36.40**	369

Table 1: Area and runtime comparisons among SP (on Sun Sparc Ultra60), O-tree (Sparc Ultra 60), B*-tree (Sparc Ultra-I), enhanced O-tree (Sparc Ultra60), CBL (Sparc 20), TCG (Sparc Ultra60) and TCG-S (Sparc Ultra60) for area optimization. The best areas are in boldface.

is a large variance in its final solutions. Based on the experimental results, we rank the convergence speed from the fastest to the slowest and the solution stability from the most stable to the least stable as follows: TCG-S $\succ$ TCG $\succ$ SP. We note that the stability and convergence speed should be very important metrics to evaluate the quality of a floorplan representation because they reveal the corresponding solution structure for optimization. However, they were often ignored in previous works. (Most previous works focus on the comparison of solution space and packing complexity. Nevertheless, we find that the solution structure induced by a representation plays an even more important role in floorplan optimization.)

Circuit	O-tree		enhanced O-tree		TCG		TCG-S	
	Wire mm	Time sec	Wire mm	Time sec	Wire mm	Time sec	Wire mm	Time sec
apte	**317**	47	**317**	15	363	2	363	2
xerox	368	160	372	39	**366**	15	**366**	6
hp	153	90	150	19	**143**	10	**143**	4
ami33	52	2251	52	177	44	52	**43**	89
ami49	636	14112	629	688	604	767	**579**	570

Table 2: Wirelength and runtime comparisons among O-tree, enhanced O-tree, TCG, and TCG-S for wirelength optimization. All ran on Sun Sparc Ultra60.

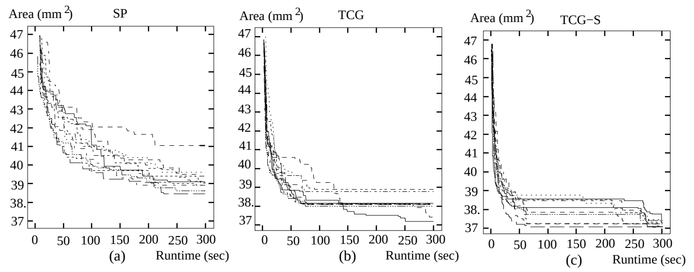

Figure 5: Comparison for stability and convergence among SP, TCG, and TCG-S for ami49.

For the experiments with boundary modules, we compared TCG-S with the SP-based method in [6] using the same data generated by [6]. The second column of Table 3 shows the numbers of the top, bottom, left, and right modules, denoted by $|T|$, $|B|$, $|L|$, and $|R|$, respectively. As shown in Table 3, TCG-S obtains smaller silicon areas than [6]. Figure 6 (right) shows the resulting placement for ami49 with boundary modules.

8 Concluding Remarks

We have presented the TCG-S representation for general floorplans by combining the advantages of two most promising P*-admissible representations TCG and SP, and at the same time eliminating their disadvantages. We also have proposed a loglinear-time packing scheme and a linear-time perturbation scheme for TCG-S. We note that these schemes can also be applied to most existing representations such as SP and BSG. Based on our theoretical study and extensive experiments, we also have shown the superior capability, efficiency, stability, and flexibility of TCG-S for floorplan design.

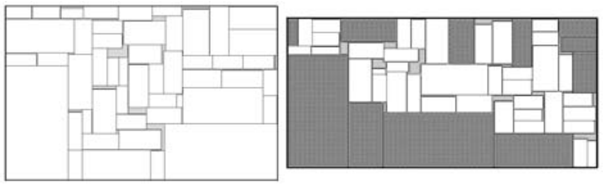

Figure 6: Resulting placements of ami49 (1) left: area optimization (area $= 36.398mm^2$); (2) right: placement with boundary modules being heavily shaded $((|T|, |B|, |L|, |R|) = (3, 3, 2, 3)$, area $= 36.765mm^2$). Note that the lightly shaded regions denote dead spaces.

Circuit	$\|T\|, \|B\|, \|L\|, \|R\|$	Lai et al. [6]		TCG-S	
		Area mm^2	Time sec	Area mm^2	Time sec
apte	1, 1, 1, 1	**46.92**	15	**46.92**	3
xerox	1, 1, 1, 1	20.4	19	**19.977**	33
hp	1, 1, 1, 1	9.24	23	**9.158**	26
ami33	2, 2, 2, 2	1.21	290	**1.190**	238
ami49	3, 3, 2, 3	36.84	601	**36.765**	584

Table 3: Area and runtime comparisons between [6] (on Pentium-II 350) and TCG-S (on Sun Sparc Ultra60) for placement with boundary modules.

References

[1] Y.-C. Chang, Y.-W. Chang, G.-M. Wu, and S.-W. Wu, "B*-trees: A new representation for non-slicing floorplans," *Proc. DAC*, pp. 458–463, 2000.

[2] T. Cormen, C. Leiserson, and R. Rivest, *Introduction to Algorithms*, McGraw-Hill Book Company, 1990.

[3] P.-N. Guo, C.-K. Cheng, and T. Yoshimura, "An O-Tree representation of non-slicing floorplan and its applications,"*Proc. DAC*, pp. 268–273, 1999.

[4] X. Hong, G. Huang, T. Cai, J. Gu, S. Dong, C.-K. Cheng, and J. Gu, "Corner Block List: An effective and efficient topological representation of non-slicing floorplan," *Proc. ICCAD*, pp. 8–12, 2000.

[5] S. Kirkpatrick, C. D. Gelatt, and M. P. Vecchi, "Optimization by simulated annealing," *Science*, vol. 220, no. 4598, May 13, 1983, pp.671–680.

[6] J.-B. Lai, M.-S Lin, T.-C Wang, and L.-C. Wang, "Module placement with boundary constraints using the sequence-pair," *ASP-DAC*, pp.515–520, 2001.

[7] E. Lawler, *Combinatorial Optimization: Networks and Matroids*, Holt, Rinehart, and Winston, 1976.

[8] J.-M Lin and Y.-W Chang, "TCG: A transitive closure graph-based representation for non-slicing floorplans," *Proc. DAC*, pp.764–769, 2001.

[9] Y. Ma, S. Dong, X. Hong, Y. Cai, C.-K. Cheng, and J. Gu "VLSI floorplanning with boundary constraints based on corner block list," *Proc. ASP-DAC*, pp. 509–514, 2001.

[10] H. Murata, K. Fujiyoshi, S. Nakatake, and Y. Kajitani, "Rectangle-packing based module placement," *Proc. ICCAD*, pp. 472–479, 1995.

[11] H. Murata, K. Fujiyoshi, and M. Kaneko, "VLSI/PCB placement with obstacles based on sequence pair," *Proc. ISPD*, pp. 26–31, 1997.

[12] S. Nakatake, K. Fujiyoshi, H. Murata, and Y. Kajitani, "Module placement on BSG-Structure and IC layout applications," *Proc. ICCAD*, pp. 484–491, 1996.

[13] R. H. J. M. Otten, "Automatic floorplan design,"*Proc. DAC*, pp.261–267, 1982.

[14] Y. Pang, C.-K. Cheng, and T. Yoshimura, "An enhanced perturbing algorithm for floorplan design using the O-tree representation," *Proc. ISPD*, pp. 168-173, 2000.

[15] K. Sakanushi and Y. Kajitani, "The quarter-state sequence (Q-sequence) to represent teh floorplan and applications to layout optimization," *Proc. Asia Pacific Conf. Circuits and Systems*, pp. 829–832, 2000.

[16] X. Tang and D. F. Wong, " FAST-SP: A fast algorithm for block placement based on sequence pair," *Proc ASP-DAC*, pp. 521–526, 2001.

[17] T.-C. Wang, Personal communication, 2001.

[18] D. F. Wong, and C. L. Liu, "A new algorithm for floorplan design," *Proc. DAC*, pp. 101–107, 1986.